CALPHAD: Computer Coupling of Phase Diagrams and Thermochemistry 56 (2017) 10–18

Contents lists available at ScienceDirect

CALPHAD: Computer Coupling of Phase Diagrams and Thermochemistry

journal homepage: www.elsevier.com/locate/calphad

Thermodynamic descriptions of the Sb/Ge unary systems

Chengliang Xu[a], Changrong Li[a,*], Shuanglin Chen[b], Cuiping Guo[a], Zhenmin Du[a], Yue Yuan[a]

[a] *School of Materials Science and Engineering, University of Science and Technology Beijing, Beijing 100083, China*
[b] *CompuTherm LLC, 8401 Greenway Blvd, Middleton, WI 53562, USA*

ARTICLE INFO

Keywords:
Sb/Ge unary system
Gibbs energy description
Murnaghan equation
P-T diagram
Calphad method

ABSTRACT

This paper focuses on the theoretical descriptions of the Gibbs energies concerning the unary systems of Antimony and Germanium. The Gibbs energy expressions of the vapor phase and the condensed phases are included in order to study the influences of temperature and pressure on the phase equilibrium status. The vapor phase is treated as a real solution of the constituent species by considering the fugacity coefficients of gas species in order to assure the reasonability of the P-T (Pressure-Temperature) diagrams at high pressure. The condensed phases are described in the light of the pressure dependent Murnaghan equation which is presented as a pressure dependent contribution G_{pres} in the present work. The pressure correction factors for the condensed phases include the molar volume, the parameters of the variations of the thermal expansivity and the compressibility with temperature, and the variation of the bulk modulus with pressure. The related parameters of the vapor phase and all the condensed phases are thermodynamically optimized for Sb and Ge unary systems, on the basis of experimental measurements in literature. The calculated results of the P-T relations and the P-V (Pressure-Volume) curves agree well with the experimental data. The calculated slope of liquid-solid coexistence curve at the low pressure of the P-T phase diagram of Sb unary system follows Clausius-Clapeyron equation. The calculated heat capacity curves of condensed phases of Sb and Ge are analyzed and discussed to assure the reasonability of the thermodynamic models described in the paper. The present thermodynamic descriptions of both unary systems are of great benefit to the preparation process of the $CoSb_3$-based thermoelectric materials, especially for the prevention of the volatilization of Sb containing vapor species and the determination of the sintering temperature under certain pressure.

1. Introduction

$CoSb_3$-based Skutterudites refer to a certain kind of thermoelectric materials with a host of doping and substituting elements in the crystal lattice sites as well as in the cage-like intrinsic crystal voids. The substitution of Germanium for Antimony in the $CoSb_3$-based Skutterudites may contribute to the enhancement of the thermoelectric properties [1–3]. In actual sintering process, the related pressure-temperature relations are greatly decisive to their phase equilibria and material preparation. At present, the thermodynamic parameters concerning the vapor phase and the condensed phases can be retrieved from PURE and SSUB databases of Thermo-Calc Software package, respectively [4]. However, the high pressure databases containing the pressure correction factors are relatively scarce according to the available literature reports.

This paper is intended to optimize the pressure-temperature phase diagrams for the unary systems of Sb and Ge, with the consideration of the pressure correction factors, so as to develop the related thermodynamic databases.

2. Thermodynamic models

2.1. The vapor phase

In terms of the vapor phases of Sb and Ge unary systems, the main species are Sb(g), Sb_2(g), Sb_3(g), Sb_4(g) and Ge(g), Ge_2(g), respectively [4]. In the present work, the real solution modeling is used for describing the Gibbs free energy of the vapor phase in order to assure the reasonability of the *P-T* diagram at high pressure, for the reason that the vapor phases will become thermodynamically stable at $P >$ 10 GPa without considering the fugacity coefficients of vapor species for both unary systems. The Gibbs energy expression of the vapor phase is shown as the following:

$$G_m^{gas}(T) = \sum y_i[{}^0G_i^{gas}(T) + RT\ln(y_i) + RT\ln(f_i/P_0)] \quad (1)$$

where y_i and ${}^0G_i^{gas}(T)$ are the molar fraction and the molar Gibbs

* Corresponding author.
E-mail address: crli@mater.ustb.edu.cn (C. Li).

http://dx.doi.org/10.1016/j.calphad.2016.11.007
Received 9 May 2016; Received in revised form 31 October 2016; Accepted 9 November 2016

energy of the species i of the vapor phase taken from the SSUB substance database [4], P_0 is the standard atmospheric pressure, R and T are the gas constant and temperature, and $f_i = f_i(P,T)$ is the fugacity of vapor species i which can be several orders of magnitude higher than P when $P > 1\times10^5$ Pa [5].

According to the previous literatures concerning the vapor fugacity, the fugacity coefficient $\gamma = \frac{f}{P}$ and its relationship with pressure and temperature can be given as the following expression [5–7]:

$$ln\gamma = \ln\left(\frac{f}{P}\right) = A \times \frac{P}{1 \times 10^5 Pa} + B \times \frac{P^2}{(1 \times 10^5 Pa)^2} (T \geq 298K) \quad (2)$$

where A and B are parameters related to temperature, and the reasonable value of A and B should be relatively small in that f should infinitely approach to P at low pressures when $P \leq 1\times10^5$ Pa.

However, there exist no available literature report concerning the exact vapor species fugacity expressions of A and B of Sb, Sb_2, Sb_3, Sb_4 and Ge, Ge_2. Particularly, the P-T relationships of Sb and Ge vapor phases are not reported at high pressures when $P > 1\times10^5$ Pa and thus the related fugacities at high pressure are not available, either. So it is necessary to approximately estimate A and B of the fugacity expressions concerning the vapor species of Sb and Ge. Based on the fugacity study of nitrogen related systems [5–7], in the present optimization work, the expression form of A and B is taken from the aforementioned literatures:

$$M = \frac{M_1}{T} + \frac{M_2}{T^2} + \frac{M_3}{T^3} \quad (3)$$

where M_1, M_2 and M_3 (M=A or B) are the undetermined coefficients on the basis of the experimental information of the vapor phase fugacity at high pressure. In terms of Sb and Ge unary systems, the following expressions are used for both Sb and Ge vapor species by analogy with nitrogen to reflect the variation of A and B with temperature approximately:

$$A = \frac{0.3926K}{T} - \frac{39.23K^2}{T^2} + \frac{2800K^3}{T^3} B = \frac{3.805 \times 10^{-6}K}{T} + \frac{0.00113K^2}{T^2} - \frac{0.07K^3}{T^3} \quad (4)$$

Provided that the fugacity coefficients of the vapor species of Sb and Ge are regarded as similar, Eq. (1) can be simplified as the following:

$$G_m^{gas}(T) = \sum y_i [{}^0G_i^{gas}(T) + RT \ln(y_i)] + RT \ln(f/P_0) \quad (5)$$

After the approximate treatment of the parameters A and B for the Sb and Ge vapor phases, the P-T relationships are reasonable at both high and low pressure ranges. The precise expressions of A and B concerning the fugacity coefficients of Sb and Ge vapor species require further practical study and discussion in future research work.

2.2. The condensed phases

The Gibbs energy of a condensed phase containing a pure element depends on both temperature and pressure. The pressure dependence of the Gibbs energy can be expressed in the form of the Murnaghan equation [8]:

$$G_{pres} = \frac{A \exp(A_0 T + A_1 T^2/2 + A_2 T^3/3)}{(K_0 + K_1 T + K_2 T^2)(n-1)} \{[1 + nP(K_0 + K_1 T + K_2 T^2)]^{1-1/n} - 1\} \quad (6)$$

where A represents the molar volume $V_m = (\frac{\partial G_m}{\partial P})_T$ of the material at a temperature of 0 K and a pressure of 0 Pa; the parameters A_0, A_1, A_2 and K_0, K_1, K_2 indicate the variation of the volume thermal expansivity $\alpha = \frac{1}{V_m}(\frac{\partial V_m}{\partial T})_P = A_0 + A_1 T + A_2 T^2$ and compressibility $\kappa = -\frac{1}{V_m}(\frac{\partial V_m}{\partial P})_T = K_0 + K_1 T + K_2 T^2$ of the condensed phase as the functions of temperature at a pressure of 0 Pa; and the parameter n is the variation of the bulk modulus with pressure $B(T,P) = B(T,0) + nP$, where $B(T,P)$ represents the bulk modulus as the function of temperature and pressure and $B(T,0)$ represents the bulk modulus at zero pressure. Taking the G_{pres} term into account, the Gibbs energy of a condensed phase containing a pure element can be expressed as the following:

$$G = a + bT + cT \ln(T) + dT^2 + eT^3 + fT^{-1} + gT^7 + hT^{-9} + G_{pres} \quad (7)$$

where a, b, c, d, e, f, g and h are the parameters of the Gibbs energy expression with no consideration of the pressure effect.

3. Experimental data

3.1. Antimony system

At $P < 1\times10^5$ Pa, there exist Rhombo_A7 Sb, liquid phase and vapor phase composed of Sb, Sb_2, Sb_3 and Sb_4 in the Antimony system. In terms of the high pressure phase of Sb, there is an academic dispute over the crystal structure of this phase. Duggin [9] and Sasaki [10] suggested the crystal structure of the high pressure phase of Sb should be Tetragonal by analogy with As and Bi. Klement [11] determined the crystal structure of the high pressure phase of Sb and suggested the reasonable structure of this phase should be closely related to Bcc_A2. However, most literatures [12–15] based on XRD method pointed out that the high pressure phase of Sb should be Monoclinic, which was derived from an orthorhombic SnS type structure. In the present optimization work, the crystal structure of the high pressure phase of Sb is regarded as Monoclinic.

The experimental data of the Antimony system is relatively abundant. Young [12] collected the unary phase diagram of Sb based on the experimental data from various literatures. Zhao [16] summarized the relationship between the saturated vapor pressure of Sb and temperature according to the original research reported by Russian experts. Besides, others [13,14,17–22] determined the phase boundaries of Rhombo_A7 Sb, Monoclinic Sb and liquid by means of thermochemical analysis, including XRD (X-Ray Diffraction), ATD (Analysis of Thermal Desorption) and DSC (Differential Scanning Calorimeter). The triple point of the three-phase equilibrium of Rhombo_A7, Monoclinic and liquid is 840 K at 5.7 GPa, while that of Rhombo_A7, liquid and vapor is 903.7 K at 20.5 Pa [11,16]. Moreover, it is reported that the linear thermal expansivity and the compressibility data of Sb turn out to be 10.5×10^{-6} /K and 23.535×10^{-12} /Pa at 20 °C, respectively, and the molar volume of Rhombo_A7 Sb at normal pressure and temperature is 1.75×10^{-5} m^3/mol [23]. In terms of liquid Sb, similarly, the compressibility data of liquid Sb is 4.33×10^{-11} /Pa at 1200 K according to sound velocity method [24]. These experimental data are used to evaluate the model parameters in the present work.

3.2. Germanium system

Germanium acts as a substitution element of Antimony in the $CoSb_3$-based materials. Compared with Sb, the experimental data of Ge are relatively scarce. There exist four phases in the Ge unary system, vapor phase, liquid phase, Diamond_A4 Ge and Tetragonal Ge. The vapor phase is composed of species Ge and Ge_2[25].

Young [12] described the high pressure condensed phase diagram of Ge based on available experimental data from literature. Menoni et al. [26], Vaidya et al. [27], Bundy [28] and Vohra et al. [29] determined the phase boundaries of Diamond_A4 Ge, Tetragonal Ge and liquid using the thermal analysis including adiabatic calorimetry, levitation method and drop calorimetry, as well as the physical measurements including elastic compression test and bulk modulus test. The triple point of the three-phase equilibrium of liquid, Diamond_A4 Ge and Tetragonal Ge, however, has not got an unanimous conclusion according to the existing report. Jayaraman [30] and

Yang [31] summarized the equilibrium relationship of these three phases, and suggested the possible triple point should be 800 K at 10.2 GPa. Vechten [32] pointed out that this triple point is about 835 K at 10.2 GPa based on Quantum Dielectric Theory. Young [12], Bundy [28] and Vohra [29] suggested the triple point be 820 K at 10.2 GPa according to their academic research. Based on all the literature reports above, this triple point is taken as 820 K at 10.2 GPa in the present optimization. No triple point concerning the three-phase equilibrium of Diamond_A4 Ge, liquid and vapor was reported. Besides, the linear thermal expansivity and the volume compressibility data are 6.0×10^{-6}/K and 12.93×10^{-12} /Pa at 20 ℃, respectively, and the molar volume of Diamond_A4 Ge at normal pressure and temperature is 1.26×10^{-5} m^3/mol [23]. Moreover, it is reported that the compressibility data of liquid Ge is 2.525×10^{-11} /Pa at 1200K by means of sound velocity method and static method [33,34]. Analogous to Sb, these experimental data are used in the present optimization of the Ge unary system.

4. Optimization results

4.1. The Sb system

As mentioned above, in the present work, the high pressure phase of Sb is treated as Monoclinic. It is generally recognized that the four phases, Rhombo_A7 Sb, Monoclinic Sb, liquid and gas, constitute the unary system of Antimony [9–22,35]. However, there exists no Monoclinic Sb in the SGTE Database. Consequently the model of this phase was constructed with the consideration of the reasonable change trend of its heat capacity at high pressures and temperatures. The parameters of the Gibbs energy expression of Monoclinic Sb were optimized on the basis of the low temperature part of $GHSER_{Sb}$, named as $GHSER_{Sb}$_Low [36] as listed in Table 1, to assure the heat capacity curve smooth at high temperature. Based on the available experimental data, the optimization work was carried out by means of Pandat 2016 software [37]. All the optimized model parameters are given in Table 1. The fugacity coefficients of gas species, γ, are regarded as the same for Sb(g), Sb_2(g), Sb_3(g) and Sb_4(g) approximately.

4.2. The Ge system

The four phases, Diamond_A4 Ge, Tetragonal Ge , the liquid phase and the vapor phase, constitute the unary system of Germanium. The SGTE database gives expressions of all the four phases under atmospheric pressure. Because of the scarcity of the experimental data and the dispersivity of the data points for the *P-T* diagram of Ge at high pressure, the data reported by Ref. [12] are given a larger weight for its comprehensiveness of the collected data. All the obtained model parameters are given in Table 2. Analogous to Sb, the fugacity coefficients of vapor species are set the same value as mentioned in Section 2.1.

5. Analysis and discussion

5.1. Antimony system

The optimization results of Sb unary system include the phase diagrams of both the high and the low pressure ranges. In order to present the whole phase diagram and the partial enlarged diagram clearly, the lg(*P*)-*T* diagram and the *P-T* diagram are shown in Fig. 1(a) and (b), respectively. The consistent results are obtained between the calculated results and the experimental data. The optimization results show that the triple point of the three-phase equilibrium of Rhombo_A7 Sb, Monoclinic Sb and liquid is about 840 K at 5.66 GPa; and that of Rhombo_A7, liquid and vapor is about 903.7 K at 20.3 Pa.

The Pressure-Volume diagram, P-V_m diagram, is of great significance to evaluate the pressure correction factors in the present optimization work. The expression of the P-V_m relationship can be given in the following equation:

$$V_m = \left(\frac{\partial G_m}{\partial P}\right)_T = \frac{A\exp(A_0 T + A_1 T^2/2)}{(1+nPK_0)^{1/n}} \tag{8}$$

As for the optimized parameters for the Gibbs energy expressions of the solid phases, the molar volume of Rhombo_A7 Sb at 0 K and 0 Pa, A_rho, is 1.65×10^{-5} m^3/mol, and the real molar volume of Rhombo_A7 at normal temperature and pressure is 1.75×10^{-5} m^3/mol, which is closely matched with the theoretical molar volume at 0 K and 0 Pa. The main contributor of the volume thermal expansivity of the Rhombo_A7 Sb, A_0_rho, turns out to be 3.01×10^{-5} /K, while the reported linear thermal expansivity at 298 K is 1.05×10^{-5} /K. These data follow closely the empirical law that the volume expansivity is about three times of the linear expansivity. Similarly, the main contributor of the volume compressibility of the Rhombo_A7 Sb, K_0_rho, is 2.13×10^{-11} /Pa, while the literature reported compressibility at 293 K is 2.3535×10^{-11} /Pa. In terms of the liquid phase, the calculated compressibility is 4.76×10^{-11} /Pa , while the literature reported compressibility at 1200K is about 4.33×10^{-11} /Pa. These data are also closely matched with each other. Based on the available pressure correction factors, the P-V_m diagram and the P-V/V_O diagram of Rhombo_A7 Sb and Monoclinic Sb are given in Fig. 2. The calculated results fit the experimental data [15] well.

Furthermore, the heat capacities of liquid Sb, Rhombo_A7 Sb and Monoclinic Sb are discussed in the present paper, in order to evaluate the reasonability of their pressure correction factors. The related heat capacity curves are shown in Fig. 3. For Rhombo_A7 Sb and liquid, with the purpose of evaluating the influence of G_{pres} terms, the heat capacity data retrieved from Pure module of Thermo-Calc software without G_{pres} terms are listed as a comparison. It is apparent that the G_{pres} term almost makes no difference concerning the heat capacities at standard atmospheric pressure. For Monoclinic Sb, it is imperative that the heat capacity should be thermodynamically meaningful at the discussed temperature and pressure scope. Meanwhile, the heat capacity curve of Monoclinic Sb should converge to the heat capacity of the liquid phase at high temperature, in order to be consistent with the SGTE standard. Consequently, we used a piecewise function to describe the characteristic of its heat capacity curve, and the curve strictly converges to the heat capacity of the liquid phase when $P=1\times10^5$ Pa, the value of which is 31.38 J/(mol .K). To investigate the reasonability of the heat capacity of Monoclinic Sb, the heat capacities of both 1×10^5 Pa and 8 GPa are given as a reciprocal comparison. The slightly descending of the heat capacity curve at 8 GPa may rely on the sharp ascending of G_{pres} term of Monoclinic Sb at high pressures, which influences the stability of Monoclinic Sb at corresponding conditions. The data mentioned above show the reasonability of the unary database of Sb.

It is worth noting that the data concerning the solidification curve of Rhombo_A7 Sb at low pressure is rarely reported. In the present work, the slope of the two-phase equilibrium curve of liquid and Rhombo_A7 Sb at low pressure, $\frac{dp}{dT}$, is estimated according to Clausius-Clapeyron equation

$$\frac{dp}{dT} = \frac{\Delta H}{T_m \Delta V_m} \tag{9}$$

where ΔH is the latent heat of sublimation of Sb, T_m the melting temperature, ΔV_m the molar volume change in the solidification process which can be approximately calculated as the following:

$$\Delta V_m = \frac{M_{Sb}}{\rho_{Sb}} \times c_{Sb} \tag{10}$$

where M_{Sb} is the molar atomic weight of Sb, ρ_{Sb} the density, and c_{Sb} the volume contraction percentage during the solidification process.

According to the literature report [38], ΔH=19875.784 J/mol,

Table 1
The optimized results of Antimony unary system.

Phase	Thermodynamic function	Pressure term/correction factor
Gas	$\ln\gamma = A \times \frac{P}{1\times10^5Pa} + B \times \frac{P^2}{(1\times10^5Pa)^2} (T \geq 298\ K)$	
	$A = \frac{0.3926K}{T} - \frac{39.23K^2}{T^2} + \frac{2800K^3}{T^3} B = \frac{3.805\times10^{-6}K}{T} + \frac{0.00113K^2}{T^2} - \frac{0.07K^3}{T^3}$	
	$GGASSB\begin{cases} = +260807.82-37.9550038T-21.27672T\ln T + 5.524195\times10^{-4}\times T^2-1.05228767\times10^{-7}\times T^3 + 9996.235\times T^{-1} (298K<T<1500K) \\ = +277520.519-132.229974T-8.970999T\ln T - 0.0030704565T^2 + 5.21558333\times10^{-8}\times T^3 - 3997436T^{-1} (1500K<T<3200K) \\ = +220721.423+26.8449864T-27.71232T\ln T - 7.8024\times10^{-4}\times T^2 + 2.46637333\times10^{-8}\times T^3 + 25565705T^{-1} (3200K<T<5700K) \\ = +181935.295+193.241235T-48.14252T\ln T + 0.0028203175T^2-8.119545\times10^{-8}\times T^3 + 25871630T^{-1} (5700K<T<9000K) \\ = +1141367.55-1326.1236T+119.631T\ln T - 0.0102407757T^2 + 1.09708933\times10^{-7}\times T^3 - 1.0049905\times10^9\times T^{-1} (9000K<T<10000K) \end{cases}$	${}^0G_{Sb}^{Gas} = GGASSB + RT\ln(10^{-5}\times P) + RT\ln\gamma$

Phase	Thermodynamic function	Pressure term/correction factor
	$GGASSB2\begin{cases} = +225644.034-1.64062093T-38.03868T\ln T + 5.08568\times10^{-4}T^2-1.31408217\times10^{-7}\times T^3 + 60968.15T^{-1} (298K<T<1700K) \\ = +231514.886-6.690928917T-38.05471T\ln T + 0.002531817T^2-4.26984\times10^{-7}\times T^3 - 2451004T^{-1} (1700K<T<3400K) \\ = +569974.061-1288.56295T+120.7968T\ln T - 0.0306031857T^2 + 8.68664667\times10^{-7}\times T^3 - 1.376966\times10^8\times T^{-1} (3400K<T<5700K) \\ = -689327.546+1714.84499T-228.6644T\ln T + 0.012556505T^2-1.31793767\times10^{-7}\times T^3 + 7.14668\times10^8\times T^{-1} (5700K<T<6000K) \end{cases}$	${}^0G_{Sb_2}^{Gas} = GGASSB2 + RT\ln(10^{-5}\times P) + RT\ln\gamma$
	$GGASSB3 = +277165.227 + 46.0530737T-58.19257T\ln T - 2.0866265\times10^{-6}\times T^2 + 8.316025\times10^{-11}\times T^3 + 43601.08\times T^{-1} (298K<T<6000K)$	${}^0G_{Sb_3}^{Gas} = GGASSB3 + RT\ln(10^{-5}\times P) + RT\ln\gamma$
	$GGASSB4 = +192849.585 + 194.765811T-83.12392T\ln T - 5.116865\times10^{-6}\times T^2 + 2.043415\times10^{-10}\times T^3 + 115767.85T^{-1} (298K<T<6000K)$	${}^0G_{Sb_4}^{Gas} = GGASSB4 + RT\ln(10^{-5}\times P) + RT\ln\gamma$
Liquid	${}^0G_{Sb}^{Liq}\begin{cases} = +19822.328-21.923164T + GHSER_{Sb} - 1.74847\times10^{-20}\times T^7 + G_{pres}liq (298K<T<903.7K) \\ = +8175.359+147.455986T-31.38T\ln T + G_{pres}liq (903.7K<T<2000K) \end{cases}$	$Aliq = 1.636\times10^{-5}$ $A_0liq = 6.965\times10^{-5}$ $A_1liq = 6.915\times10^{-10}$ $K_0liq = 4.76\times10^{-11}$ $Nliq = 8$
Rhombo_A7	${}^0G_{Sb}^{Rhom\ boA7} = GHSER_{Sb} + G_{pres}rho$	$Arho = 1.65\times10^{-5}$ $A_0rho = 3.01\times10^{-5}$ $A_1rho = 1.26\times10^{-10}$ $K_0rho = 2.13\times10^{-11}$ $Nrho = 10$
Monoclinic	$GHSER_{Sb}Low = -9242.858 + 156.154689T - 30.5130752T\ln T + 0.007748768T^2 - 3.003415\times10^{-6}T^3 + 100625T^{-1}\ (298.15K<T<6000K)$	
	${}^0G_{Sb}^{Monoclinic}\begin{cases} = +23056-56.96T+4.86T\ln T + 8.56\times10^{-3}T^2 - 1.66\times10^{-7}T^3 + 360007T^{-1} + 9.06\times10^{23}T^{-9} + GHSER_{Sb}Low + G_{pres}mon (298K<T<1875K) \\ = -1505.221457+170T-31.38T\ln T + G_{pres}mon\ (1875K<T<5000K) \end{cases}$	$Amon = 1.675\times10^{-5}$ $A_0mon = 1.56\times10^{-5}$ $A_1mon = 8.62\times10^{-9}$ $K_0mon = 1.21\times10^{-10}$ $Nmon = 8$

Table 2
The optimized results of Germanium unary system.

Phase	Thermodynamic function	Pressure term/correction factor
Gas	$\ln\gamma = A \times \frac{P}{1\times10^5 Pa} + B \times \frac{P^2}{(1\times10^5 Pa)^2} (T \geq 298\ K)$ $A = \frac{0.3926K}{T} - \frac{39.23K^2}{T^2} + \frac{2800K^3}{T^3}$ $B = \frac{3.805\times10^{-6}K}{T} + \frac{0.00113K^2}{T^2} - \frac{0.07K^3}{T^3}$ $GGASGE \begin{cases} = +354205.659 + 120.562507T - 43.82842T\ln T + 0.01399744T^2 - 1.669525\times10^{-6}\times T^3 + 250845.65T^{-1} (298K < T < 1100K) \\ = +373131.148 - 56.1903326T - 18.6573T\ln T - 0.0010641577T^2 + 4.18049833\times10^{-8}\times T^3 - 2447580T^{-1} (1100K < T < 4900K) \\ = +296853.328 + 145.237519T - 42.45872T\ln T + 0.00233340125T^2 - 5.148525\times10^{-8}\times T^3 + 44812690T^{-1} (4900K < T < 10000K) \end{cases}$	${}^0G_{Ge}^{Gas} = GGASGE + RT\ln(10^{-5}\times P) + RT\ln\gamma$
	$GGASGE2 \begin{cases} = +452821.305 + 129.510905T - 58.27585T\ln T + 0.015550048T^2 - 2.367595\times10^{-6}\times T^3 + 381719.4T^{-1} (298K < T < 900K) \\ = +466026.197 - 21.0297748T - 36.10521T\ln T - 0.00115536605T^2 + 1.43478617\times10^{-8}\times T^3 - 1107859T^{-1} (900K < T < 4000K) \\ = +448161.895 - 8.64280187T - 36.8412T\ln T - .0021332445T^2 + 8.26510333\times10^{-8}\times T^3 + 14926150T^{-1} (4000K < T < 6000K) \end{cases}$	${}^0G_{Ge_2}^{Gas} = GGASGE2 + RT\ln(10^{-5}\times P) + RT\ln\gamma$
Liquid	${}^0G_{Ge}^{Liq} \begin{cases} = +37141.49 - 30.687043T + GHSER_{Ge} + 8.56632\times10^{-21}\times T^7 + G_{pres}liq (298K < T < 900K) \\ = +37141.489 - 30.687044T + GHSER_{Ge} + 8.56632\times10^{-21}\times T^7 + G_{pres}liq (900K < T < 1211.4K) \\ = +27243.473 + 126.324186T - 27.6144T\ln T + G_{pres}liq (1211.4K < T < 3200K) \end{cases}$	$Aliq = 9.676\times10^{-6}$ $A_0 liq = 3.56\times10^{-6}$ $A_1 liq = 6.01\times10^{-10}$ $K_0 liq = 2.61\times10^{-11}$ $Nliq = 6$
Phase	Thermodynamic function	Pressure term/correction factor
Tetragonal	${}^0G_{Ge}^{Teteagonal} \begin{cases} = +19313.847 + 149.135573T - 29.5337682T\ln T + 0.005568297T^2 - 1.513694\times10^{-6}T^3 + 163298T^{-1} + G_{pres}tet (298K < T < 900K) \\ = +23110.761 + 86.36087T - 19.8536239T\ln T - 0.003672527T^2 + G_{pres}tet (900K < T < 1211.4K) \\ = +19251.796 + 140.208024T - 27.6144T\ln T - 8.59809\times10^{28}T^{-9} + G_{pres}tet (1211.4K < T < 3000K) \end{cases}$	$Atet = 9.9\times10^{-6}$ $A_0 tet = 1.27\times10^{-5}$ $A_1 tet = 5.69\times10^{-9}$ $K_0 tet = 5.56\times10^{-11}$ $Ntet = 5$
Diamond_A4	${}^0G_{Ge}^{Diamond} = GHSER_{Ge} + G_{pres}dia$	$Adia = 1.049\times10^{-5}$ $A_0 dia = 1.86\times10^{-5}$ $A_1 dia = 1.86\times10^{-9}$ $K_0 dia = 1.36\times10^{-11}$ $Ndia = 5$

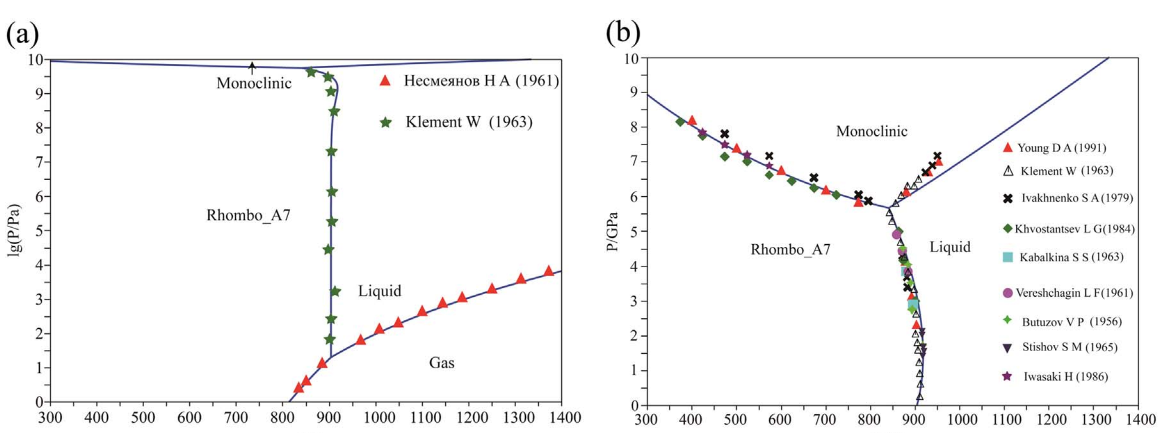

Fig. 1. The optimized phase diagram of Sb system compared with experimental data: (a) The lg(P/Pa)-T/K global diagram; (b) The enlarged partial diagram.

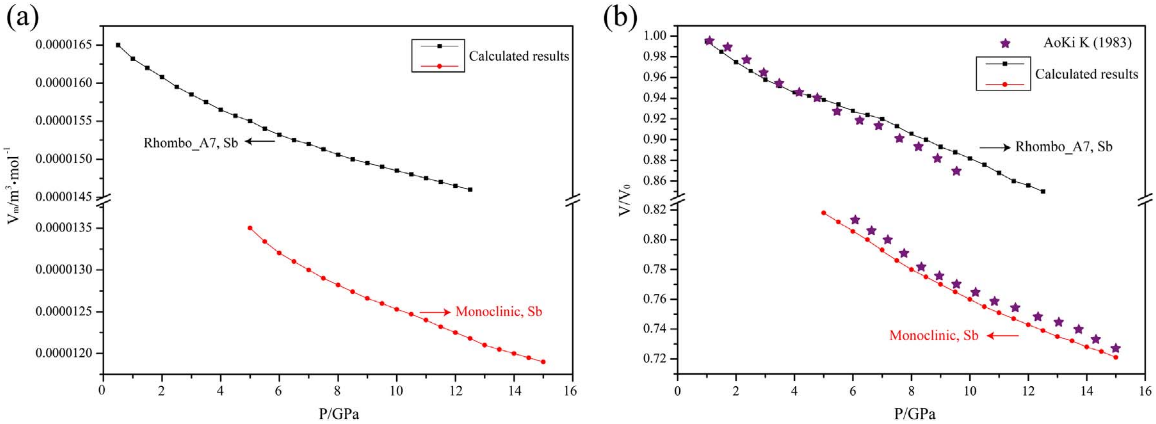

Fig. 2. The calculated Pressure-Volume diagrams of Rhombo_A7 Sb and Monoclinic Sb: (a) The calculated P-V_m diagram; (b) The calculated P-V/V_O diagram compared with experimental data.

T_m=903.7 K, M_{Sb}=0.12175 kg/mol, ρ_{Sb}=6697 kg/m^3, and c_{Sb}=0.79%, the calculated result shows that the slope of the two-phase equilibrium curve of the liquid and Rhombo_A7 Sb is 1.53×10^8 Pa/K. This value is supported by the related literature [11] and is very close to the present calculation using the optimized thermodynamic parameters, as shown in Fig. 4.

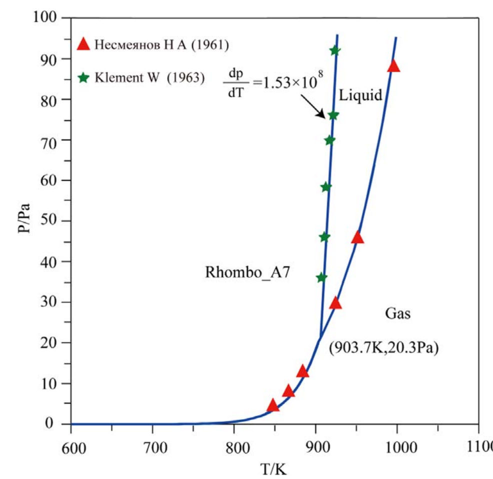

Fig. 4. The P-T phase diagram of Sb at low pressure compared with experimental data.

5.2. Germanium system

The experimental data of Ge unary system from literature are merely confined to high pressure ranging from 1 to 20 GPa. The lg(P)-T and the P-T phase diagrams are shown in Fig. 5(a) and (b), respectively. The triple point of the three-phase equilibrium of Diamond_A4 Ge, Tetragonal Ge and liquid is about 818 K at 10.1 GPa according to the present optimization result.

According to the optimized results, the molar volume of Diamond_A4 Ge at 0 K and 0 Pa, A_dia, is 1.049×10^{-5} m^3/mol, and the real molar volume of Diamond_A4 Ge at normal temperature and pressure is 1.26×10^{-5} m^3/mol. The two values are approximate with each other. The main contributor of the volume thermal expansivity of Diamond_A4 Ge, A_0_dia, is 1.86×10^{-5} /K, while the reported linear thermal expansivity at 293 K is 6.0×10^{-6} /K, close to 1/3 of the volume thermal expansivity. Meanwhile, the main contributor of the compressibility of Diamond_A4 Ge, K_0_dia, is 1.36×10^{-11} /Pa, while the literature reported value of volume compressibility at 293 K is 1.293×10^{-11} /Pa. For liquid Ge, the calculated compressibility is 2.61×10^{-11} /Pa , while the literature reported compressibility at 1200 K is about 2.525×10^{-11} /Pa. With the available pressure correction factors, the P-V_m diagram and the P-V/V_O diagram of Diamond_A4 Ge and Tetragonal Ge are given in Fig. 6. The calculated results fit the experimental data [26,39] well.

Analogous to Sb, the heat capacities of liquid, Diamond_A4 Ge and Tetragonal Ge are discussed in the present work, in order to evaluate the reasonability of the pressure correction factors concerning these three phases. The related heat capacity curves are shown in Fig. 7, in which the G_{pres} term almost makes no difference concerning the heat capacities of liquid and Diamond_A4 Ge at standard atmospheric pressure. In terms of Tetragonal Ge, the heat capacities of both 1×10^5 Pa and 16 GPa are given in Fig. 7(b). The calculated results

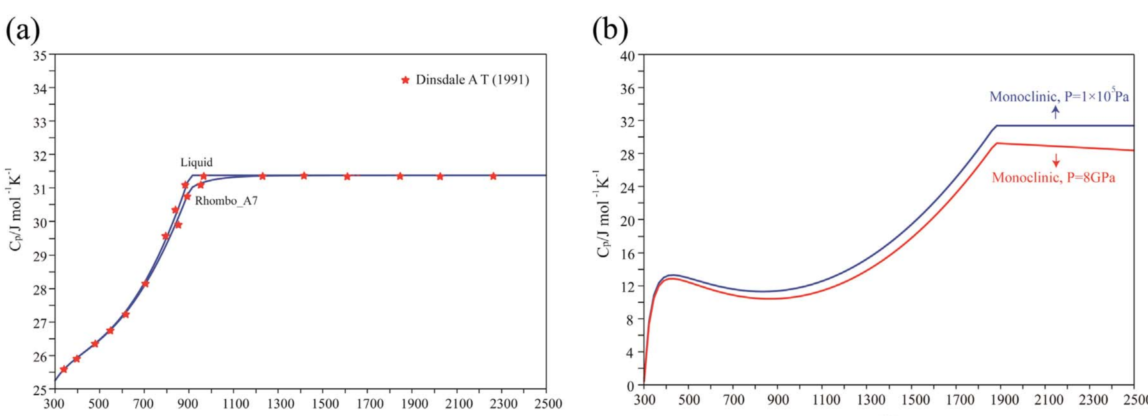

Fig. 3. The calculated heat capacity curves of liquid, Rhombo_A7 Sb and Monoclinic Sb: (a) The calculated heat capacities of Rhombo_A7 Sb and liquid Sb compared with model input; (b) The calculated heat capacities of Monoclinic Sb at P=1×10^5 Pa and 8 GPa.

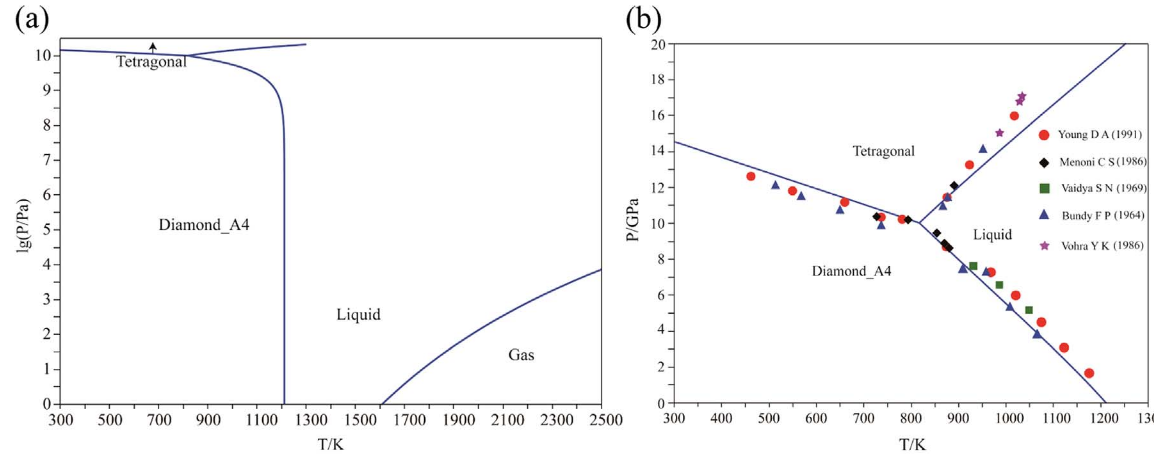

Fig. 5. The optimized phase diagram of Ge system compared with experimental data: (a) The lg(P/Pa)-T/K global diagram; (b) The enlarged partial diagram.

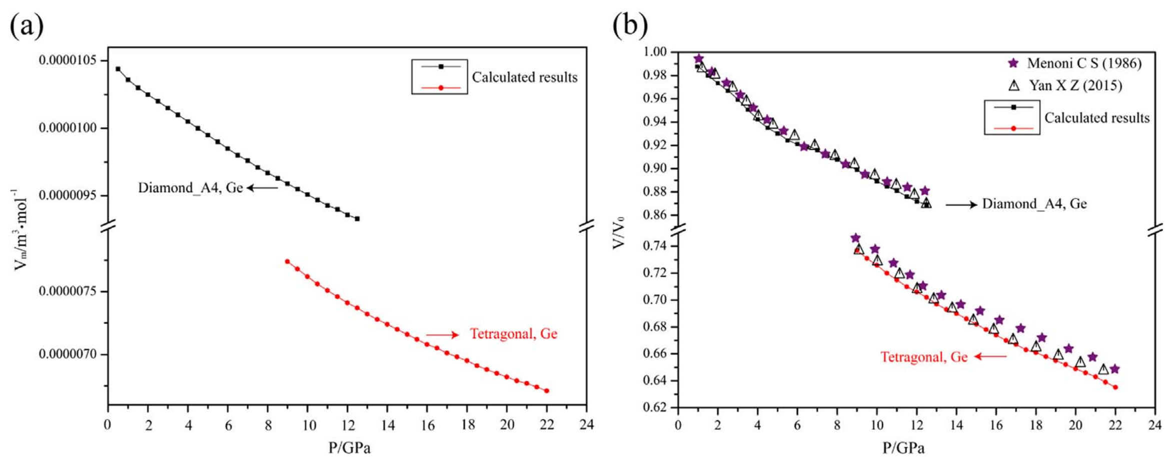

Fig. 6. The calculated Pressure-Volume diagrams of Diamond_ A4 Ge and Tetragonal Ge: (a) The calculated P-V_m diagram; (b) The calculated P-V/V_O diagram compared with experimental data.

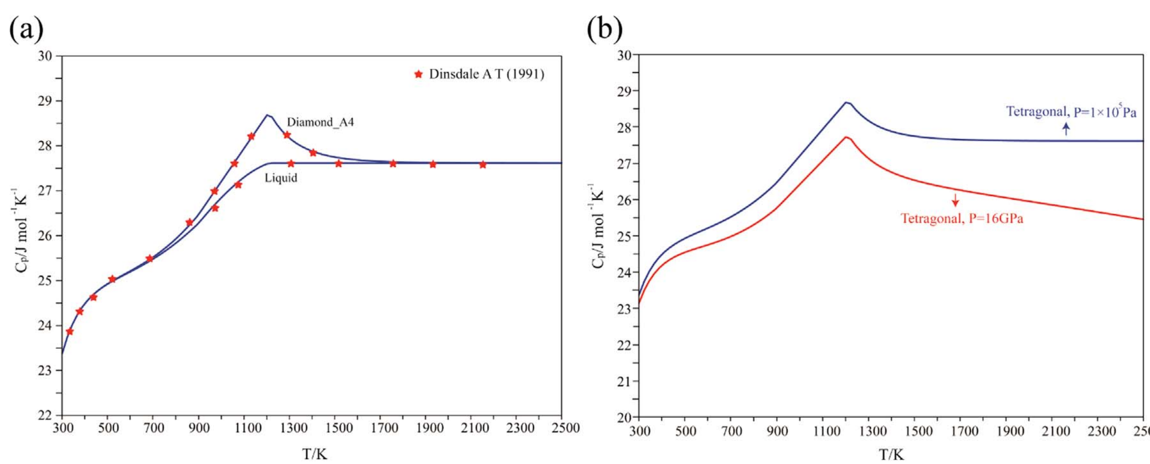

Fig. 7. The calculated heat capacity curves of liquid, Diamond_A4 Ge and Tetragonal Ge: (a) The calculated heat capacities of Diamond_A4 Ge and liquid Ge compared with model input; (b) The calculated heat capacities of Tetragonal Ge at P=1×10^5 Pa and 16 GPa.

mentioned above show the reasonability of the unary database of Ge.

5.3. The discussion of the application of the databases

The volatilization of Sb shows a prominent influence on the preparation of $CoSb_3$-based thermoelectric materials [40]. In the sintering process of the $CoSb_3$-based Skutterudites, the pressure condition is nearly vacuum or argon filled, and the temperature range is controlled from 873 to 973 K or even lower [41–43] in case of the oxidation of the metal substrate. In the present work, the contributions of G_{pres} of the condensed phases to the corresponding total Gibbs Energies are calculated, as shown in Figs. 8 and 9. Fig. 8 gives the variation of G_{pres} with pressure at 298.15 and 2000 K, showing that when $P < 10^8$ Pa, the G_{pres} term is relatively small, while when P becomes to 10^8 Pa or even higher, the G_{pres} term contributes so significantly that it can no longer be neglected. Fig. 9 gives the variation

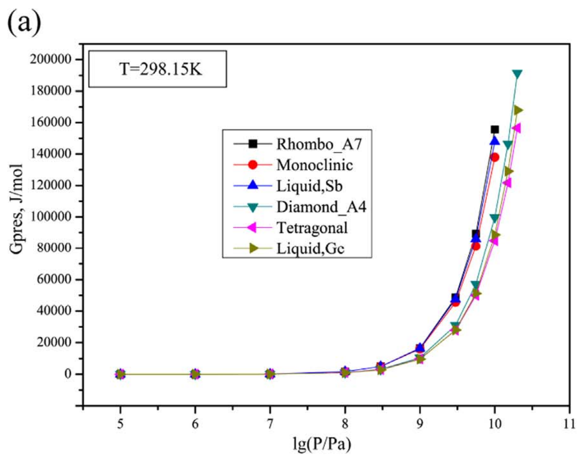

Fig. 8. The G_{pres}-lg(P) relationship of Sb and Ge: (a) T=298.15 K; (b) T=2000 K.

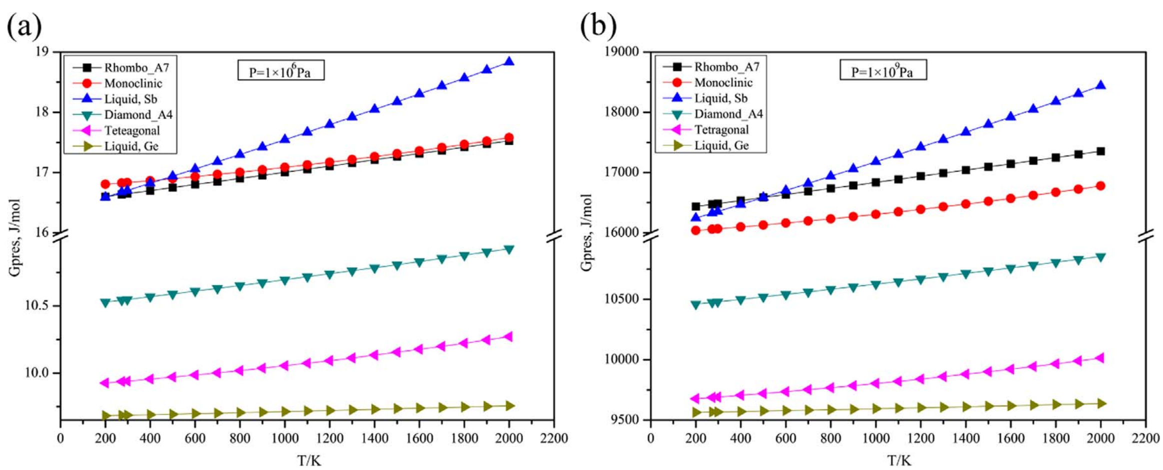

Fig. 9. The G_{pres}-T relationship of Sb and Ge: (a) P=10^6 Pa; (b) P=10^9 Pa.

of G_{pres} with temperature at 10^6 and 10^9 Pa, and it can be noticed that the influence of T on G_{pres} term takes on a monotone increasing trend with the increase of temperature. Taking account of both *P* and *T*, it can draw a conclusion that the G_{pres} term can no longer be neglected when *P* and *T* become high enough.

It is the theoretical law that the saturated vapor pressure of a certain substance increases with the ascending of temperature. For this reason, the sintering temperature cannot be set too high to reach a high saturated vapor pressure and a high pyrolysis of the substance. However, the sintering temperature cannot be set too low either to increase the difficulty caused by atomic diffusion and reaction kinetics to merely guarantee the high vacuum during the sintering process. Thus, it can be suggested that a number of Sb particles be added when the $CoSb_3$-based Skutterudites are sealed in the closed environment. The Sb particles may decompose and volatilize, and the vapor species, Sb(g), Sb_2(g), Sb_3(g) and Sb_4(g), may contribute to the increase of the system pressure and to the prevention of the volatilization of Sb in the $CoSb_3$-based substrate. Containing the Gibbs energy parameters of Sb and Ge for the vapor phase and the condensed phases, the thermodynamic database of the $CoSb_3$-based materials will be helpful to calculate the added amount of Sb particles in the sintering process, and be more important to analyze the phase equilibrium relations under different temperatures and pressures as well.

6. Conclusions

The Gibbs energy expressions of the unary systems of Antimony and Germanium including the fugacity coefficients of the vapor phases and the pressure correction factors for the condensed phases are thermodynamically optimized. The experimental results, especially the data concerning the molar volume, the volume thermal expansivity and compressibility of both elements, serve as the vital reference basis in the optimization process. Using the thermodynamic data obtained in the present work, the two-phase equilibrium curves, the three-phase equilibrium points and the *P*-*T* phase diagrams are calculated. The calculated slope of the two-phase equilibrium curve of liquid and Rhombo_A7 Sb at low pressure follows Clausius-Clapeyron equation. The calculated phase diagrams and the Pressure-Volume curves agree well with the experimental phase equilibrium data. Meanwhile, the heat capacities of the calculation results are thermodynamically meaningful at the discussed temperature and pressure scope. The thermodynamic data of the unary systems of Sb and Ge can provide an essential basis for the thermodynamic database of the $CoSb_3$-based thermoelectric materials. In addition, the form of G_{pres} model used in the present work can be widely used when other unary systems associated with the pressure dependent condensed phases are concerned.

Acknowledgements

This work was supported by National Key Research and Development Program of China (No. 2016YFB0701201) and National Natural Science Foundation of China (No. 51271027). Thanks to the CompuTherm LLC, USA for supplying the Pandat 2016 software.

Appendix A. Supplementary material

Supplementary data associated with this article can be found in the online version at http://dx.doi.org/10.1016/j.calphad.2016.11.007.

References

[1] G.S. Nolas, C.A. Kendziora, H. Takizawa, J. Appl. Phys. 94 (2003) 7440–7444.
[2] G.S. Nolas, J. Yang, H. Takizawa, Appl. Phys. Lett. 84 (2004) 5210.
[3] G.A. Lamberton Jr, R.H. Tedstrom, T.M. Tritt, et al., J. Appl. Phys. 97 (11) (2005) 113715.
[4] Thermo-Calc Software, Thermo-Calc Database Guide, Royal Institute of Technology, Stockholm, 2008.
[5] B. Onderka, J. Unland, R. Schmid-Fetzer, J. Mater. Res. 17 (12) (2002) 3065–3083.
[6] J. Unland, B. Onderka, A. Davydov, et al., J. Cryst. Growth 256 (1–2) (2003) 33–51.
[7] X.Y. Ma, C.R. Li, W.J. Zhang, et al., Calphad 29 (3) (2005) 247–253.
[8] A.T. Dinsdale, Calphad 15 (4) (1991) 317–425.
[9] M.J. Duggin, J. Phys. Chem. Solids 33 (6) (1972) 1267–1271.
[10] T. Sasaki, K. Shindo, K. Niizeki, Solid State Commun. 67 (6) (1988) 569–572.
[11] J.W. Klement, A. Jayaraman, G.C. Kennedy, Phys. Rev. 131 (2) (1963) 632–637.
[12] D.A. Young, Phase Diagrams of the Elements, University of California Press, California, 1991.
[13] S.S. Kabalkina, T.N. Kolobyanina, L.F. Vereshchagin, Sov. Phys. JETP 13 (2) (1970) 259–263.
[14] H. Iwasaki, T. Kikegawa, Physica B+C. 139 (1986) 259–262.
[15] K. Aoki, S. Fujiwara, M. Kusakabe, Solid State Commun. 45 (2) (1983) 161–163.
[16] T.C. Zhao, Antimony, Metallurgical Industry Press, Beijing, 1987.
[17] S.A. Ivakhnenko, Y.G. Ponyatovskiy, Fiz. Metalloved. 47 (6) (1979) 1314–1316.
[18] S.S. Kabalkina, L.F. Vereshchagin, V.P. Mylov, Dokl. Akad. Nauk SSSR 152 (3) (1963) 585.
[19] L.F. Vereshchagin, A.A. Semercham, H.H. Kuzin, et al., Dokl. Akad. Nauk. SSSR 136 (2) (1961) 320–321.
[20] L.G. Khvostantsev, V.A. Sidorov, Physica Status Solidi (a) 82 (2) (1984) 389–398.
[21] S.M. Stishov, N.A. Tikhomirova, Sov. Phys. JETP 48 (1965) 1215.
[22] V.P. Butuzov, E.G. Poniatovsky, G.P. Shakhovskoy, Dokl. Akad. Nauk SSSR 109 (3) (1956) 519–520.
[23] I.S. Grigoriev, E.Z. Meilikhov, A.A. Radzig, Handbook of Physical Quantities, CRC Press, Florida, 1997.
[24] M. Emuna, Y. Greenberg, E. Yahel, et al., J. Non-Cryst. Solids 362 (1) (2014) 1–6.
[25] S. Li, R.J. Van Zee, W. Weltner Jr, J. Chem. Phys. 100 (10) (1994) 7079–7086.
[26] C.S. Menoni, J.Z. Hu, I.L. Spain, Phys. Rev. B 34 (1) (1986) 362–368.
[27] S.N. Vaidya, J. Akella, G.C. Kennedy, J. Phys. Chem. Solids 30 (6) (1969) 1411–1416.
[28] F.P. Bundy, J. Chem. Phys. 41 (12) (1964) 3809–3814.
[29] Y.K. Vohra, K.E. Brister, S. Desgreniers, et al., Phys. Rev. Lett. 56 (18) (1986) 1944–1947.
[30] A. Jayaraman, W. Klement, G.C. Kennedy, Phys. Rev. 130 (6) (1963) 2277–2283.
[31] C.C. Yang, Q. Jiang, Scr. Mater. 51 (11) (2004) 1081–1085.
[32] V., J.A. Vechten, Phys. Rev. B 7 (4) (1973) 1479–1507.
[33] M. Hayashi, H. Yamada, N. Nabeshima, et al., Int. J. Thermophys. 28 (1) (2007) 83–96.
[34] T. Masaki, T. Itami, Jaxa Res. Dev. Rep. 4 (2005) 46–48.
[35] J. Kordis, K.A. Gingerich, J. Phys. Chem. 58 (11) (1973) 5141–5149.
[36] Y.B. Zhang, C.R. Li, Z.M. Du, et al., Calphad 32 (2008) 56–63.
[37] K.S. Wu, S.L. Chen, F. Zhang, et al., J. phase equilibria Diffus. 30 (5) (2009) 571–576.
[38] A.J.H. Boerboom, H.W. Reyn, H.F. Vugts, et al., Physica 30 (12) (1964) 2137–2142.
[39] X. Yan, D. Tan, X. Ren, et al., Appl. Phys. Lett. 106 (17) (2015) 171902.
[40] J.W. Sharp, E.C. Jones, R.K. Williams, et al., J. Appl. Phys. 78 (2) (1995) 1013–1018.
[41] P. Amornpitoksuk, H.X. Li, J.C. Tedenac, et al., Intermetallics 15 (4) (2007) 475–478.
[42] L.D. Dudkin, N.K. Abrikosov, Sov. Phys. Solid State 1 (2) (1959) 126–133.
[43] S. Katsuyama, M. Shichijo, M. Ito, et al., J. Appl. Phys. 84 (12) (1998) 6708–6712.